J Supercond Nov Magn (2013) 26:1991–1995
DOI 10.1007/s10948-012-1920-7

ORIGINAL PAPER

Magnetism in Double Perovskites

T. Saha-Dasgupta

Received: 7 November 2012 / Accepted: 30 November 2012 / Published online: 20 December 2012

Abstract Double-perovskite compounds with general formula $ABB'O_6$, have attracted a lot of attention in recent years due to a variety of properties exhibited by them. In this paper, we will review our recent study on a number of double-perovskite compounds, namely La-doped Sr_2FeMoO_6, Cr-based family of compounds, Sr_2CrXO_6 (X = W, Re, Os), characterized with spectacularly high ferromagnetic transition temperatures and the magneto-capacitive compound, La_2NiMnO_6, We will discuss the signature of hybridization-driven antiferromagnetism in La-doped Sr_2FeMoO_6, while the parent compound, Sr_2FeMoO_6, is a half-metallic ferromagnet. The magnetism in the 3d–5d double perovskite Sr_2CrXO_6 (X = W, Re, Os) is found to be driven by the interplay of the hybridization-driven mechanism and the superexchange, which resulted into progressive increase of T_c as one moves from W to Re to Os at the B′ site. Our work, in the context of La_2NiMnO_6, identifies its superexchange-driven microscopic origin being responsible for the near room-temperature insulating ferromagnetic behavior.

Keywords Double perovskite · Ferromagnetism · Antiferromagnetism · Electronic structure

1 Introduction

Double-perovskite oxides, $A_2BB'O_6$ where A is alkaline-earth or rare-earth metal and B and B′ are transition metals, have been widely investigated. These materials are specially interesting in view of the possibility that B and B′ cations can be ordered at the octahedral sites. Ordering is favored by large differences in ionic radii and formal charge of B and B′ cations [1, 2]. In the ordered arrangement it consists of corner sharing BO_6 and $B'O_6$ octahedra which alternate along three cubic axes. A cations sit in the hollow formed by BO_6 and $B'O_6$ octahedra (see Fig. 1). These compounds depending on the choice of B and B′ cations, show vast variety of electrical and magnetic properties, namely, metallicity, half-metallicity, insulating as well as ferromagnetism (FM), ferrimagnetism (FIM), antiferromagnetism (AFM) [1, 2]. This family of compounds has provided materials of high technological applications, namely material for spintronics application (Sr_2FeMoO_6) [3], multiferroic material (Bi_2NiMnO_6) [4], magnetodielectric materials (La_2NiMnO_6, La_2CoMnO_6) [5], possible materials for magneto-optic devices (Sr_2CrWO_6, Sr_2CrReO_6, Sr_2CrOsO_6) [6]. In this paper, we will take up a few of these compounds and will review the origin of the diverse magnetic and electronic behavior, obtained using first-principles density functional theory (DFT)-based calculations.

2 Antiferromagnetism in La-Doped Sr_2FeMoO_6

One of the very widely studied compounds in the class of double perovskites is Sr_2FeMoO_6. The attention was focused in this compound due to the proposed half-metallic character with high FM Curie temperature, opening up the possibility of room-temperature spintronics application [4]. The high Curie temperature found in this material is counter-intuitive since the magnetic ion Fe^{3+} in Sr_2FeMoO_6 is in $3d^5$ configuration, resulting into half-filled manifold of 3d, which should interact antiferromagnetically through the superexchange path of Fe–O–Mo–O–Fe. Contrary to this simple expectation, FM was found to be established through

T. Saha-Dasgupta (✉)
S.N.Bose National Centre for Basic Sciences, Kolkata, India
e-mail: tanusri@bose.res.in

hybridization-driven mechanism [7]. Within this mechanism, Mo t_{2g} energy levels, which are energetically placed within the spin split energy levels of Fe d's, attain a negative spin polarization through hybridization between Mo t_{2g} and Fe t_{2g} levels, which in turn stabilizes the parallel alignment of spins in Fe sublattice. Figure 2 shows the schematics of the hybridization-driven negative spin polarization of Mo bands as well as the effective Wannier function representation of the conduction band. The Wannier function, shown in Fig. 2, has the central character of Fe t_{2g} degrees of freedom while the tails are shaped accordingly to symmetries of Mo t_{2g} and O p, highlighting the hybridization between Mo t_{2g} and Fe t_{2g} degrees of freedom.

The above described hybridization-driven mechanism can be viewed as two sublattice double exchange model, where large classical spin is provided by Fe $S = 5/2$ spin and the mobile spin is given by the conduction electron aligned antiparallel to the classical spin, and delocalized over the Mo–Fe network. The pertinent question to ask is whether the same mechanism can also give rise to AFM. If so, one may have the possibility of designing AFM metals which are rare in nature. In order to probe this possibility, we doped the parent compound, Sr_2FeMoO_6 with La, which resulted into electron doping the system. Interestingly, our density functional theory-based [8, 9] total-energy calculations, as presented in Fig. 3, showed that beyond a critical doping of La, the system favors AFM alignment of Fe spins, compared to FM alignment as in parent compound.

The computed density of states shows AFM phase is metallic with finite density of states at Fermi level. The stabilization of AFM phase over the FM phase upon increasing La doping can be rationalized through the schematic diagram presented in Fig. 4. The left hand panel of the figure shows the schematic diagram of the density of states (DOS) close to the Fermi energy (E_f) in the FM configuration, while that in the right hand panel shows the DOS in the AFM configuration. The FM DOS in the majority spin channel consists of the empty highly localized Mo t_{2g} bands resulting in a highly peaked, narrow density of states and in the minority spin channel, which consists of the Fe–Mo hybridized dispersive conduction band. Upon doping with La, more and more electrons are introduced in the system, which increasingly populates the dispersive band in the minority spin channel, thereby progressively pushing E_f towards the edge of the narrow peaked band in the majority spin channel. At a certain doping level, the situation becomes such that the doped electron starts populating highly peaked narrow Mo t_{2g} bands. It is at this point FM becomes unstable, since in such situation it becomes energetically favorable instead to adopt to AFM configuration, in which the electron is capable to gain kinetic energy through hopping processes in both spin channels.

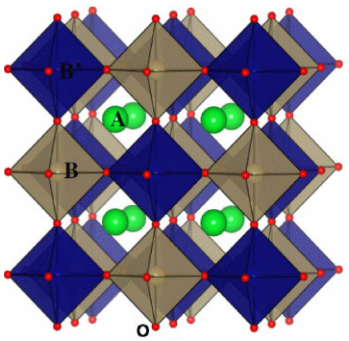

Fig. 1 Crystal structure of $A_2BB'O_6$ double perovskite

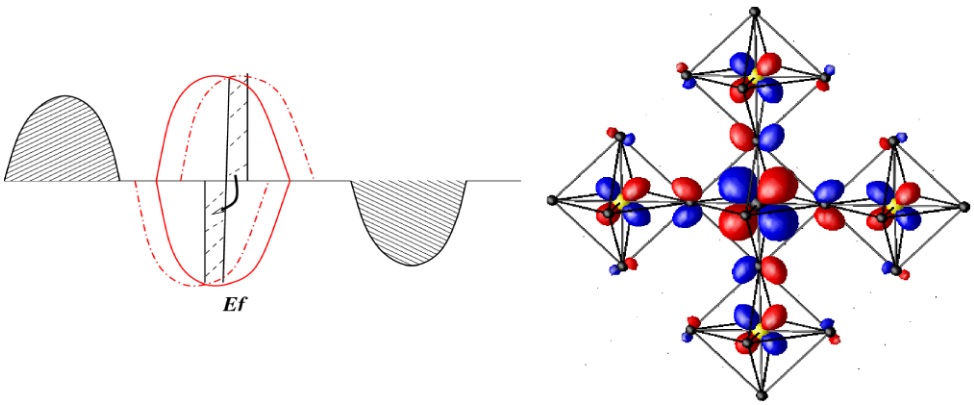

Fig. 2 *Left panel*: Schematic diagram showing the hybridization induced negative spin polarization of Mo bands for Sr_2FeMoO_6. The spin split Fe bands are shown as shaded semicircular density of states, while Mo bands are shown as semicircular density of states, marked in *red* (the density of states before switching on the hybridization is shown in *solid lines*, while that after switching on the hybridization is shown in *dashed line*). E_f marks the position of Fermi energy. *Right panel*: Effective Wannier function plot for the conduction band showing the hybridization between the central Fe site and the neighboring Mo sites. Two opposite lobes of the functions are colored as *red* and *blue* (Color figure online)

3 Origin of Magnetism and T_c Trend in Cr-Based 3d–5d Double Perovskites

For technological purpose, it is desirable to have double perovskites with even higher T_c than that reported for Sr_2FeMoO_6 [3]. Cr-based double-perovskite series, $Sr_2CrB'O_6$ (B′ = W, Re, Os), holds promise in this respect. The measured T_c for Sr_2CrWO_6, Sr_2CrReO_6 and Sr_2CrOsO_6 are reported to be ∼450–550 K [3], 635 K and ∼720 K [10, 11], respectively. It is interesting to note that in moving from CrW to CrRe to CrOs systems, more and more electrons are introduced in the system, as W, Re and Os in their 5+ valence state (considering 3+ valence of Cr) are in $5d^1$, $5d^2$ and $5d^3$ configurations, respectively. In view of the discussion presented in the preceding section on La-doped Sr_2FeMoO_6, this progressive increase of FM T_c is highly counter-intuitive, since within the framework on hybridization-driven mechanism, an increase of conduction electrons should weaken FM and finally would yield the AFM solution to be favorable. This brings in the question, whether it is hybridization-driven mechanism that is operative within the Cr-based 3d–5d series too [12]. Insets in Fig. 5, shows the plot of the effective Wannier functions corresponding to the conduction band for CrW, CrRe and CrOs compounds. As is clearly evident hybridization between Cr and B′ site becomes progressively weaker as one moves from CrW to CrRe to CrOs, evident in terms of weaker weights of the tails sitting at neighboring Cr sites surrounding the central W/Re/Os site. Concomitant to this, another interesting evolution happens in the electronic structure of Cr-B′ series. The energy level diagram of Cr and B′-t_{2g} levels in absence (shown in left half) of hybridization between the two and the renormalized B′ levels (shown in right half) after switching on the hybridization between the two is shown in Fig. 5. In all cases, the B′-t_{2g} levels appear in between the spin split energy levels of Cr-t_{2g} levels, and upon switching on the hybridization, the spin splitting at B′ site gets renormalized, satisfying the basic criteria of the hybridization induced FM. It is, however, interesting to notice that considering the bare spin splitting B′ t_{2g} levels, while the splitting for W is negligibly small, that for Re and Os are found to be ∼0.3 eV and ∼0.5 eV, respectively, suggesting the presence of a growing intrinsic, local moment at B′ site in moving from W to Re to Os compound, driven by the de-hybridization effect. This intrinsic moment at B′ site interacts with the spin at Cr site through usual superexchange process. The magnetism in Cr-B′ series, therefore, needs to be understood as the interplay of

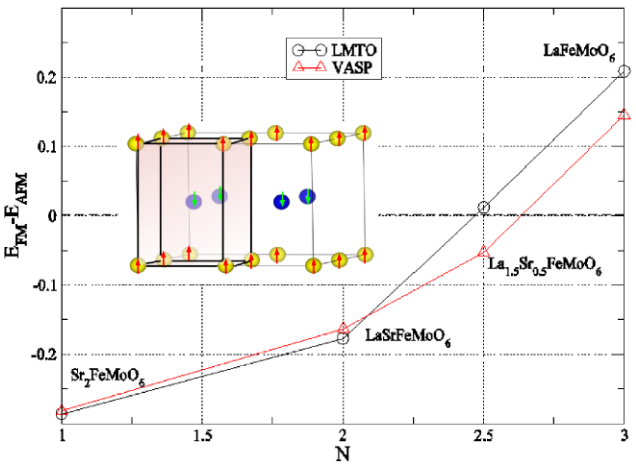

Fig. 3 Energy difference of the FM and AFM alignment of Fe spins in Sr_2FeMoO_6 and La-doped Sr_2FeMoO_6 compounds, plotted as a function of number of conduction electrons (N). N varies between 1 to 3, for 0 to 100 % doping of La. The *inset* shows the AFM arrangement of Fe spins. Results are shown for two choices of electronic structure methods, linear muffin-tin orbital (LMTO) and plane-wave-based Vienna Abinito Simulation Package (VASP) [8, 9]

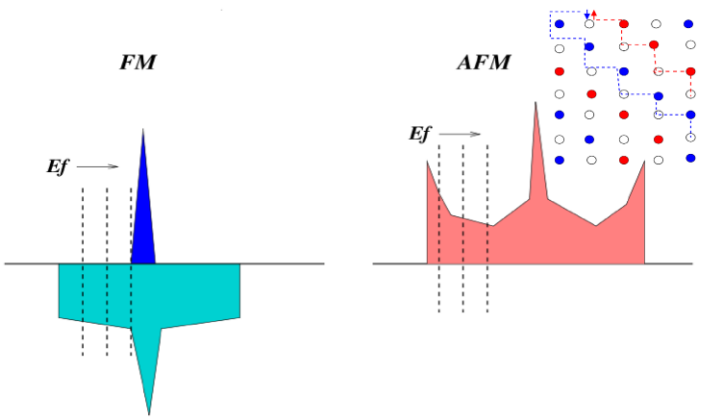

Fig. 4 Schematic DOS corresponding to FM and AFM configurations. The progressive shifting of Fermi energy in a rigid band manner is shown with *dashed lines*. In the AFM configuration, the up and down spin conduction electrons are restricted to hop to only to down and up-spin Fe sublattices, as shown the *inset* (*solid circles* denoting Fe sites and open circles denoting Mo sites, *red*/*blue* color representing up/down spin Fe sublattices), giving rise to the three peaked structure of the DOS (Color figure online)

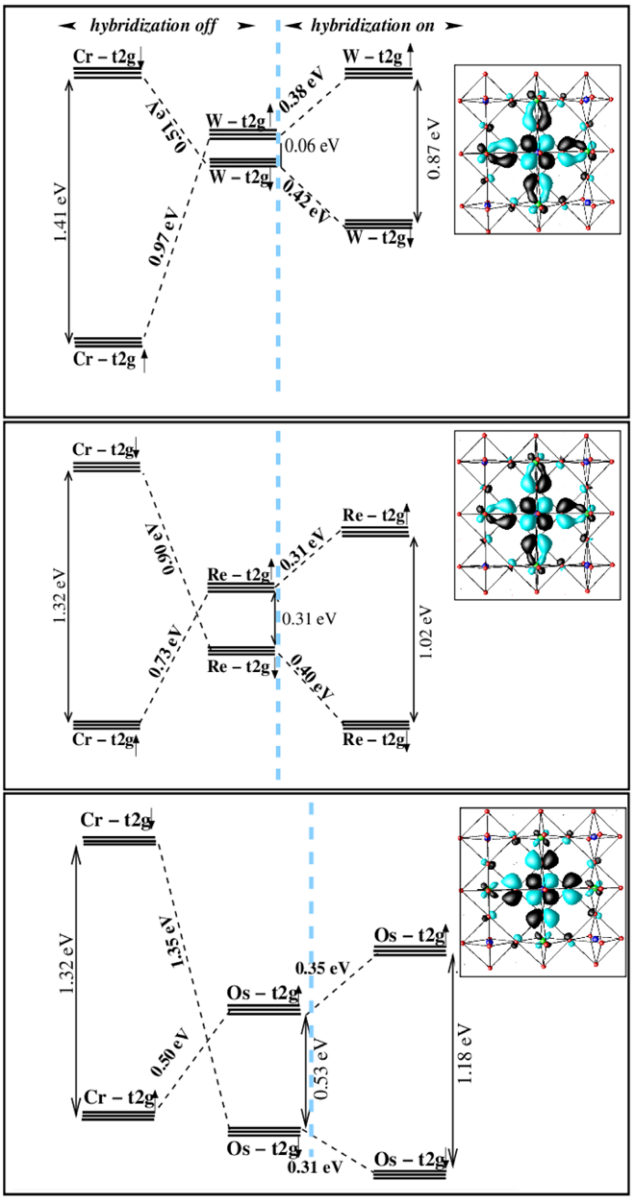

Fig. 5 The energy levelsplitting of Cr-t_{2g} and B′-t_{2g} (B′ = W, Re, Os in the *top*, *middle* and *bottom panel*) before switching on the hybridization between the two and renormalized level splitting at B′ site after switching on the hybridization. *Insets* in each panel shows the plot of the effective Wannier function corresponding to the conduction band

two mechanisms: the hybridization-driven mechanism, as operative in Sr_2FeMoO_6 and the superexchange mechanism. Hybridization-driven mechanism gets weaker as one moves along the series from W to Re to Os compound, due to the increased energy level separation of B′ from Cr. Superexchange, on the other hand, gets stronger in moving from Sr_2CrWO_6 to Sr_2CrReO_6 to Sr_2CrOsO_6 due to the presence of growing intrinsic moment at B′ site, explaining the counter-intuitive T_c trend in the Cr-B′ series.

4 Near Room-Temperature Ferromagnetic, Insulating Behavior of La_2NiMnO_6

La_2NiMnO_6 double perovskite has been reported [5] to exhibit a FM, insulating behavior with a magnetic transition temperature of ∼280 K. Generally, FM semiconductors/insulators are rare and those which are known exhibit magnetic ordering only at very low temperature. The report of near room-temperature T_c for La_2NiMnO_6, on the other hand, opens up the possibility of building devices with commercially available solid-state thermo-electric coolers. The electronic structure calculations [13] carried out within DFT established 2+ and 4+ valences of Ni and Mn, with $3d^8$ and $3d^3$ configurations, respectively. The octahedral environment of oxygen atoms, surrounding Ni and Mn splits the d levels in t_{2g} and e_g blocks, the crystal field splitting at Mn site being smaller than the spin splitting and that at Ni site being larger than the spin splitting. This leaves Ni t_{2g} states to be filled in both spin channels, Ni e_g states being half-filled while Mn t_{2g} states are half-filled with Mn e_g state being empty in both spin channels. The net magnetic interaction in La_2NiMnO_6 compound therefore, arises due to competing nature of two superexchange processes, as shown in Fig. 6: (a) superexchange process between half-filled Ni-e_g and half-filled Mn-t_{2g} states, which is AFM in nature and (b) superexchange process between half-filled Ni-e_g and empty Mn-e_g states, which is FM due to the presence of Hund's rule coupling, J_H.

The net magnetic interaction, $J_{Ni–Mn}$, therefore, can be written as the sum of the two contributions, in terms of Ni-e_g–Mn-e_g hopping interaction (t_{e-e}), Ni-e_g–Mn-t_{2g} hopping interaction (t_{t-e}), the energy level separations of Ni-e_g–Mn-e_g (Δ_{e-e}) and Ni-e_g–Mn-t_{2g} (Δ_{t-e}), choice of U and J_H values. Ab-initio estimates of t_{e-e}, t_{t-e}, Δ_{e-e} and Δ_{t-e} [13] show the net interaction to be of FM nature and of value 4–7 meV, depending on the choice of U parameter, fixing J_H at 0.9 eV. We note that t_{t-e} is non-zero due to the tilting of the NiO_6 and MnO_6 octahedra, which makes Ni–O–Mn angle 155°, deviating from 180°. While Ni-e_g–Mn-e_g hopping is an order of magnitude larger compared to Ni-e_g–Mn-t_{2g} hopping, energetically the Ni-e_g levels lie much closer to Mn t_{2g} compared to Mn-e_g.

5 Summary

In summary, our study indicates that double-perovskite compounds, with tunability of both B and B′ cations, as opposed to single B cation as in simple perovskite compound, offer a variety of magnetic properties, driven by interplay of different driving mechanisms of magnetism. The change in chemical composition of B and B′ cations affect the magnetic properties in a drastic manner. It is interesting to note

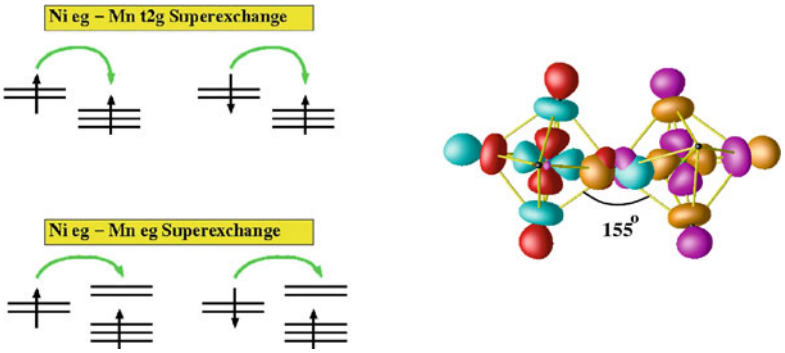

Fig. 6 *Left panel*: AFM and FM superexchange paths between Ni e_g spin ($S = 1$) and Mn t_{2g} spin ($S = 3/2$) and Ni e_g spin ($S = 1$) and empty Mn e_g. *Right panel*: Overlap of Ni e_g and Mn e_g Wannier functions, building the superexchange path through overlapping tails at the intervening O site

$$J_{Ni-Mn} = 4\frac{\sum_{m,m'}(t_{e^m,t^{m'}})^2}{(U+\Delta_{e,t})} - 4\frac{\sum_{m,m'}(t_{e^m,e^{m'}})^2 J_H}{(U+\Delta_{e,e}-J_H)(U+\Delta_{e,e})} \qquad t_{e,e} = 0.20eV \quad t_{e,t} = 0.02eV \quad \Delta_{e,e} = 1.90eV \quad \Delta_{e,t} = 0.25eV$$

that first-principles calculations are capable of capturing the effect of chemistry rather nicely, thereby providing microscopic understanding of the observed magnetic behavior. The understanding thus provided will be useful for optimization of known double perovskite and prediction of new double perovskites with improved magnetic properties.

Acknowledgements The author gratefully acknowledges contributions of H. Das, P. Sanyal, U.V. Waghmare and D.D. Sarma for the study presented here.

References

1. Anderson, M.T., Greenwood, K.B., Taylor, G.A., Poeppelmeier, K.R.: B-cation arrangements in double perovskites. Prog. Solid State Chem. **22**, 197–233 (1993)
2. Philipp, J.B. et al.: Structural and doping effects in the half-metallic double perovskite A_2CrWO_6 (A = Sr, Ba, and Ca). Phys. Rev. B **68**, 144431 (2003)
3. Kobayashi, K.I., Kimura, T., Sawada, H., Tokura Y, T.K.: Room-temperature magnetoresistance in an oxide material with an ordered double-perovskite structure. Nature **395**, 677–680 (1998)
4. Shimakawa, Y., Azuma, M., Ichikawa, N.: Multiferroic compounds with double-perovskite structures. Materials **2011**, 153–168 (2011)
5. Rogado, N.S., Li, J., Sleight, A.W., Subramanian, M.A.: Magneto-capacitance and magnetoresistance near room temperature in a ferromagnetic semiconductor: La_2NiMnO_6. Adv. Mater. **17**, 2225–2227 (2005)
6. Das, H., De-Raychaudhury, M., Saha-Dasgupta, T.: Moderate to large magneto-optical signals in high T_c double perovskites. Appl. Phys. Lett. **92**, 201912 (2008)
7. Sarma, D.D., Mahadevan, P., Saha-Dasgupta, T., Ray, S., Kumar, A.: Electronic structure of Sr_2FeMoO_6. Phys. Rev. Lett. **85**, 2549–2552 (2000)
8. Andersen, O.K., Jepsen, O.: Explicit, first-principles tight-binding theory. Phys. Rev. Lett. **53**, 2571–2574 (1984)
9. Kresse, G., Furthmüller, F.: Efficient iterative schemes for ab initio total-energy calculations using a plane-wave basis set. Phys. Rev. B **54**, 11169–11186 (1996)
10. Kato, H., Okuda, T., Okimoto, Y., Tomioka, Y., Takenoya, Y., Ohkubo, A., Kawasaki, M., Tokura, Y.: Metallic ordered double-perovskite Sr_2CrReO_6 with maximal Curie temperature of 635 K. Appl. Phys. Lett. **81**, 328–330 (2002)
11. Krockenberger, Y. et al.: Phys. Rev. B **75**, 020404-020407 (2007)
12. Das, H., Sanyal, P., Saha-Dasgupta, T., Sarma, D.D.: Origin of magnetism and trend in T_c in Cr-based double perovskites: interplay of two driving mechanisms. Phys. Rev. B **83**, 104418 (2011)
13. Das, H., Waghmare, U.V., Saha-Dasgupta, T., Sarma, D.D.: Electronic structure, phonons, and dielectric anomaly in ferromagnetic insulating double perovskite La_2NiMnO_6. Phys. Rev. Lett. **100**, 186402 (2008)